33RD CONGRESS
OF THE INTERNATIONAL COUNCIL
OF THE AERONAUTICAL SCIENCES
STOCKHOLM, SWEDEN, 4-9 SEPTEMBER, 2022

ICAS 2022 SWEDEN

IMPROVING STALL CHARACTERISTICS OF UCAV WING WITH VORTEX GENERATORS

Peter Eliasson[1], Arhur Rizzi[2], Jesper Oppelstrup[2] & Mengmeng Zhang[3]

[1]Saab, SE-581 88 Linköping, Sweden
[2]KTH, Royal Institute of Technology, Sweden
[3]Airinnova AB, Stockholm, Sweden

Abstract

Recent Unmanned Combat Air Vehicle (UCAV) configurations have not-so-slender wings with moderate leading-edge sweepangles of 45° to 60°. Planforms vary from pure delta to diamond and even lambda more or less blended wing bodies with a relatively small thickness ratio at the inner wing/fuselage region. The performance and low-observable signature considerations require a compromise between a small radar cross-section and lifting surface shapes for long range and sufficient agility. The airflow is governed largely by the progression of vortices shed from the wing leading edge which interact and produce non-linear aerodynamics. Like early swept wing fighters like the Saab 32 the UCAV may exhibit undesirable flying characteristics over part of the envelope with tip stall and pitch-up. Such problems were mitigated by vortex control "devices" like leading edge fences and notches which violate the low observable requirement. The AVT-181 SACCON is a well studied case. We attempt to improve its stalling characteristics by mimicking the leading edge fence action by a configuration of very small vortex generators and study their effect by CFD.

Keywords: vortex generator, vortex control, UCAV, not-so-slender wings, CFD, leading edge separation, Ram's horn vortex

1. Introduction

The design of UCAV wings continues to be a major research and development activity. Missions require efficient high-speed flight, loiter and good stability and handling at low speeds. Figure 1 shows the x45A, x47Z, Taranis, and SACCON. The SACCON tailless, lambda-shaped flying wing configuration is a common research UCAV concept with a 53° swept wing with parallel edges for low radar signature. It was initially defined by the NATO STO Task Group AVT-161 [1] as a benchmark for CFD methods and wind tunnel experiments.

In addition to higher tip loading, sweep sets up a velocity component along the wing that thickens the boundary layer towards the tip. Both effects make the tip prone to premature flow separation, and ultimately pitch-up [2]. The SACCON exhibits adverse stability and control characteristics at low speed and high lift (i.e. poor stalling characteristics). Since C_m is more sensitive to changes in pressure distribution than e.g. C_L, Fig. 2 displays the moment curve with streamline visualizations from incidence 14 to 18 degrees at the kink in the moment curve.

The vortical flow development responsible for the moment variation is shown in detail in Fig. 3, left. Streamline families have been selected to clarifythe interaction. At moderate incidence the flow at the wing tip separates from the surface, and as incidence increases, the stall spreads inboard ($\alpha = 15^\circ$ and $\alpha = 17^\circ$). At the same time a vortex is shed from the wing apex that spreads outboard, and ultimately interacts with the inward spreading tip vortex ($\alpha = 19^\circ$) to create chaotic flow over the aileron with loss of control authority and pitch-up. Tip stall can occur asymmetrically to generate a roll moment, and if the ailerons lie in separated flows they may have insufficient authority to control the roll.

The surface streamlines in Fig. 3, right, indicate the onset locations of the different vortices.

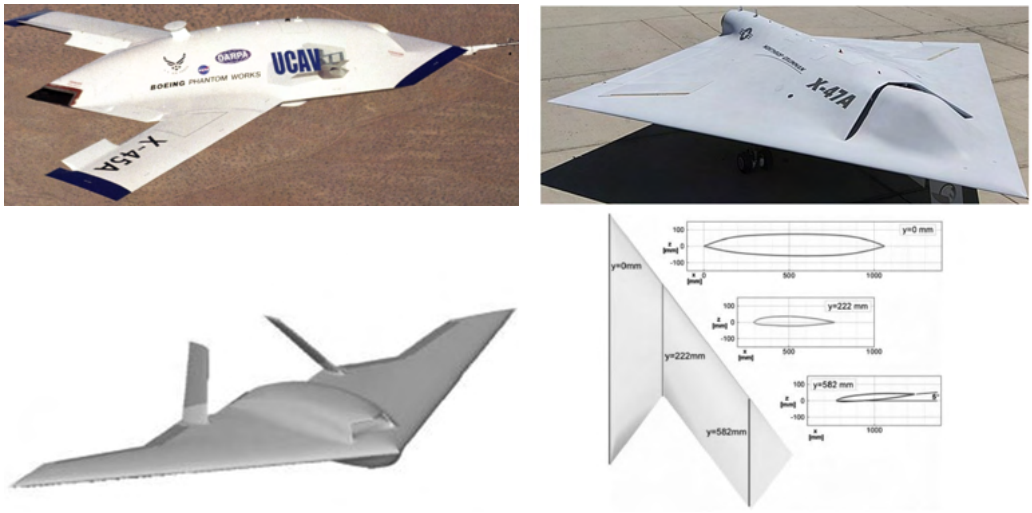

Figure 1 – Top: UCAV examples x45A, x47A. Bottom: left, future UCAV configuration, right, AVT-161 SACCON WT model

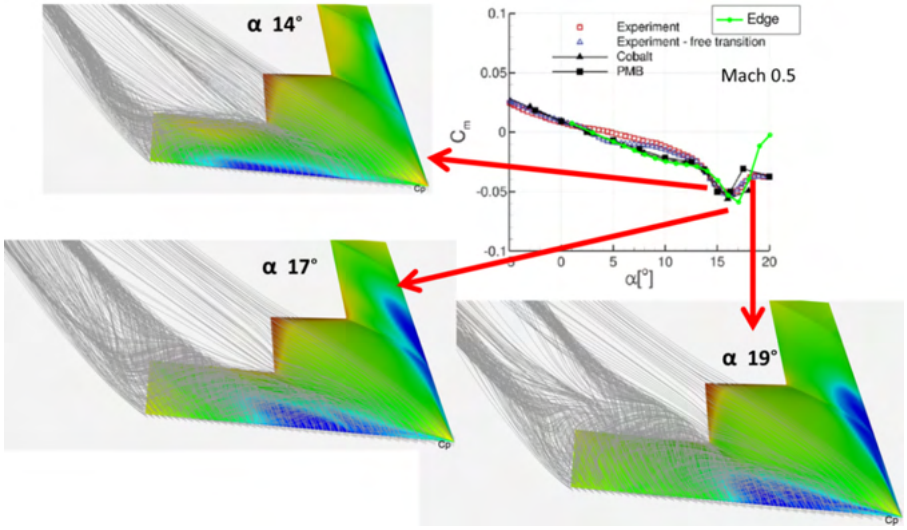

Figure 2 – Pitching moment coefficient and flow visualization for the clean SACCON configuration: streamlines over surface C_p contours; $M_\infty = 0.5$

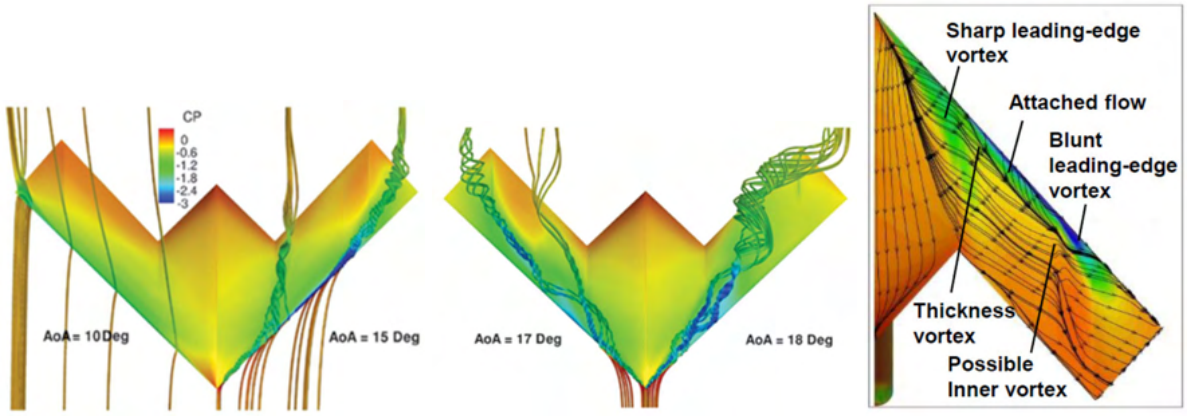

Figure 3 – Left:Vortex flow progression over SACCON α $10 - 18°$. Right: vortex system footprint surface streamlines, from [9].

2. Vortex control to mitigate stall problem

The stall problems ubiquitous for swept wings are created by the movement of the leading edge vortices at increasing incidence.
The SACCON wing has a complex planform with twist and leading edge radius variation. The flow pattern is dominated by two vortices that change onset locations with α and ultimately interact and break down. Fig. 3.

2.1 Swept wing fighter Saab 32

A very similar leading-edge vortex phenomenon occurs on the swept-wing fighters of early fifties such as the Saab 32 with wing sweep 35°, [3], Fig, 4.

Figure 4 – The Saab 32 M 1 fighter, maiden flight 1952. Note the leading edge fence.

Fig. 5 shows the development with increasing angle of attack on the Saab 32. The initial leading edge laminar separation bubble becomes a spiral by the spanwise flow. At higher α the vortex lifts off and swings aft forming a "Ram's horn" leaving the tip in separated flow.

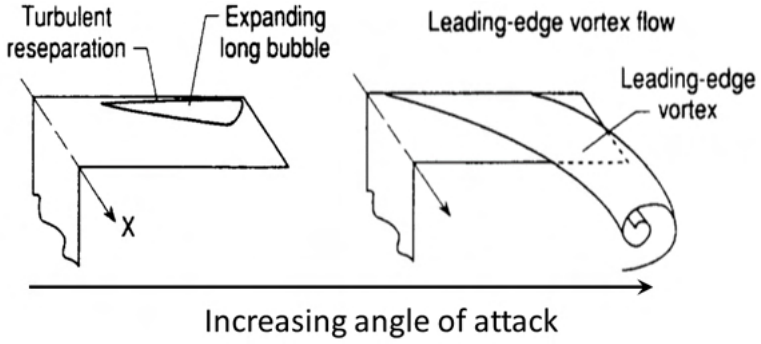

Figure 5 – Vortical flow development with increasing incidence on swept wing.

After much flight testing, various alleviating measures were devised to delay separation or at least make it predictable. The most common among these are vortex control devices, namely "stall fences", leading-edge notches, saw-teeth, leading-edge root extensions LERX, and rows of small vortex generators (VGs) [4]. Most of these work by producing vortices as the leading edge fence depicted in Fig. 6 that interact with the vortical flow over the wing to improve its characteristics. But their precise functioning is not easily predicted and must be studied by computation or experiment in each specific case. The poor stalling characteristics of the Saab 32 wing were significantly improved by adding a stall fence called a "vortex splitter" to the wing. To illustrate how the fence beneficially controls the vortex patterns, a series of RANS computations are made with the M-Edge code for the wing with and without fence for different flow speeds and angles of attack (α), see Fig. 7 for results at $M_{\infty} = 0.4$. The inset surface chordwise pressure profile at 75 % shows the strongly increased lift created by the stall fence stabilization of the outboard flow.

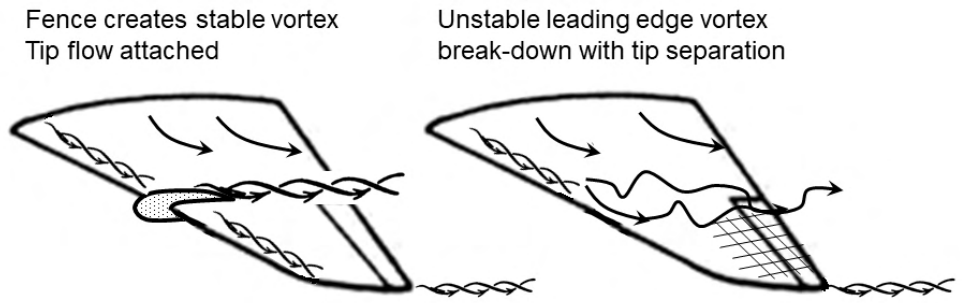

Figure 6 – Leading edge fence stabilizes and splits leading edge vortex.

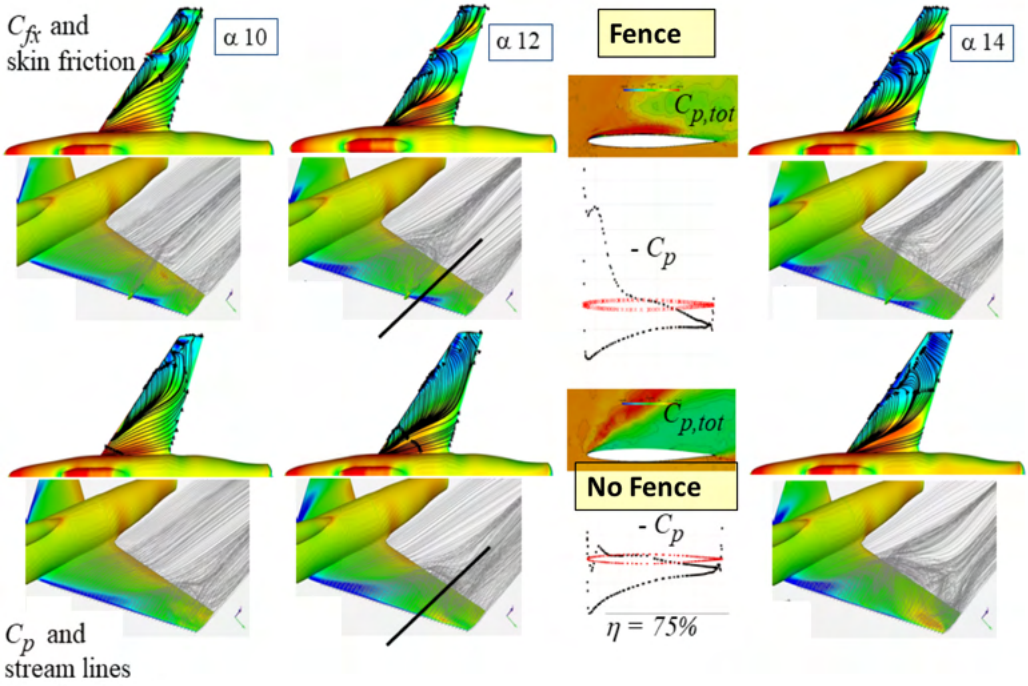

Figure 7 – Fence effect on vortices. Top, fence, bottom no fence. Right wing surface streamlines over x-component of skin friction, left wing streamlines over C_p-contours.

The fence effectively separates the vortical region near the tip from that inboard, inhibiting the apex vortex from interacting with the tip vortex. Thus the fence moderates the nonlinear variation in C_m over the alpha sweep.
As a computational experiment, the fence was replaced by a row of VGs at the same spanwise position, figure 8. Notice that at $\alpha = 8^\circ$ the VGs produce the same effect as the fence (the $\star$ symbol).

2.2 Testing VG on the SACCON

The fences on the Saab 32 cannot be used on the SACCON because of the low observable requirement. We investigate by CFD how rows of small VGs can improve the SACCON stalling characteristics. The VGs are imagined to work in the same way as for Saab 32 in Fig. 7. They hold apart the apex vortex from the tip vortex so that they do not interact as strongly as they do in Fig. 3.
The diagrams of lift and pitching moment versus angle of attack α in Figure 9 show that there is more lift from $\alpha \geq 17^\circ$ with the VGs and less upturn of C_m so slightly better stall and reduced pitch-up.
The flow visualizations with and without VGs at $\alpha = 17^\circ$ in Fig. 9 reveal the effect of VGs to control the vortices, namely they strengthen the inboard vortex and weaken the tip vortex and through this mechanism they unload the tip a little. Note that VGs are applied to the right wing only, as the leading

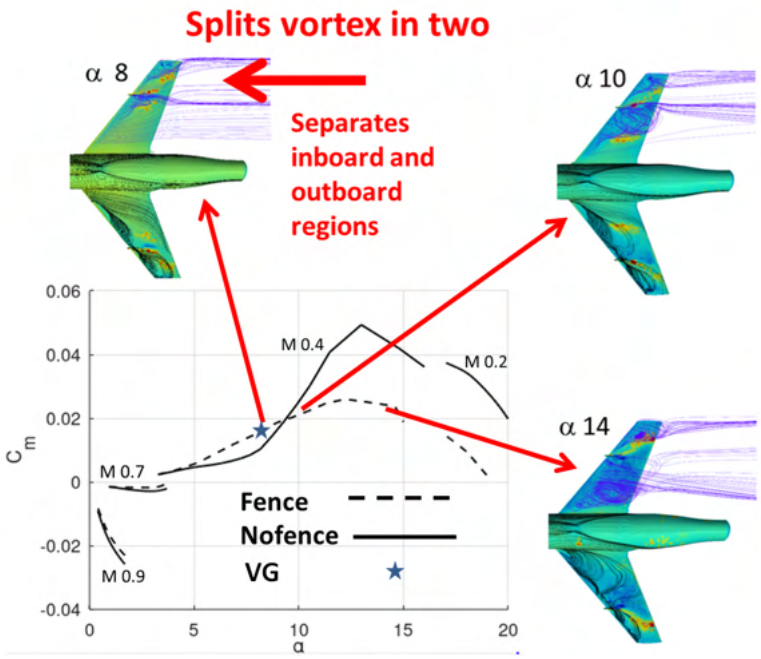

Figure 8 – Moment curves for Saab 32 wing with and without leading edge fence. Flow visualization with fence: streamlines over surface C_p contours (right wing) and skin-friction lines over contours of x-component of skin-friction vector (left wing). Star symbol shows that VGs have similar effect as fence. $M_\infty = 0.5$

edge suction peak pattern shows.

3. jBAY VG model in CFD code M-Edge

Vortex generators are on a much smaller geometry scale than wing profiles so it natural to model their effect using only a clean wing computational grid. Several such VG models for CFD codes exist and we use the jBAY model developed in [6] as an extension of the BAY model, [8]. The model applies volume forces in the computational cells occupied by the VG, idealized as a plane surface positioned on the wing surface. The force direction $\mathbf{l}$ in cell i is normal to local stream and the direction in the VG surface pointing out from wing surface, Fig. 10.
The magnitude of the force is estimated from VG area S_{VG} and dynamic pressure,

$$\mathbf{L}_i = CS_{VG}\left(V_i/\sum V_k\right)\alpha\rho|U^2|\hat{\mathbf{l}} \tag{1}$$

V_i is the volume of cell i and the sum is over all cells intersected by the VG surface. C is a tuning parameter which can roughly be estimated from lift on a flat plate. A factor $\cos\alpha$ is multiplied on to correct for high angle of attack.
Computed flows with the model are compared with a gridded solution in Fig. 11
The model has been implemented in the M-Edge compressible flow CFD package that originates from the Edge flow solver, [10]. M-Edge has been used for most of the flow simulations in the paper. It is further described in [11].

3.1 VG arrangements

The VG's should create a vortex lifting off the surface. VG pairs are convergent or divergent in the stream direction. The convergent pairs tend to create uplift between them and downdraft outside, and the divergent pairs the converse, as shown in Fig. 12, adapted from [5].
Several arrangements were tried , Fig. 13, all with VG 3 cm long and 1 cm high, convergent, angled 15°. The top right position gave the largest effect on the moment curve.

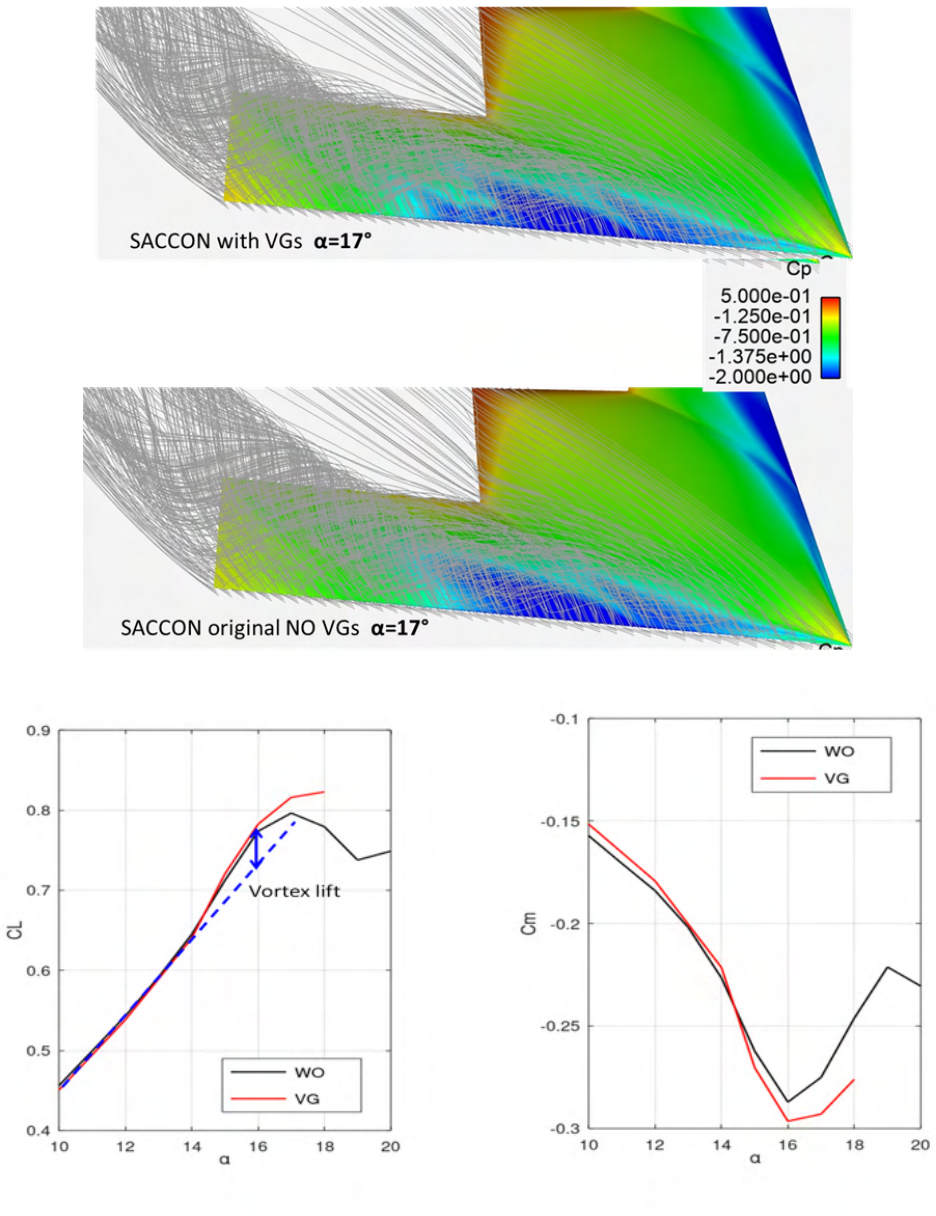

Figure 9 – Top: Streamlines and surface C_p over SACCON at α 17°, with and without VG. Bottom left: Lift curves, right : Moment curves, at M_∞ 0.5.

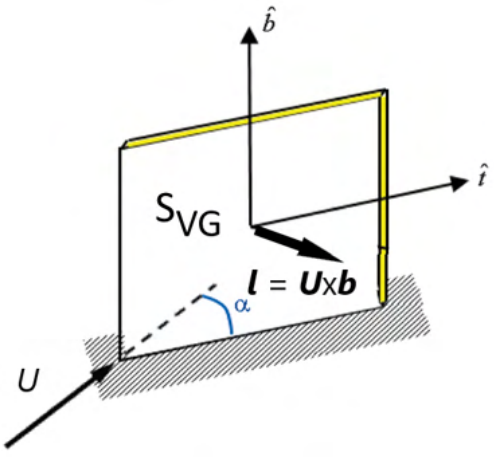

Figure 10 – Vortex generator with direction vectors and oncoming stream parallel to wing surface.

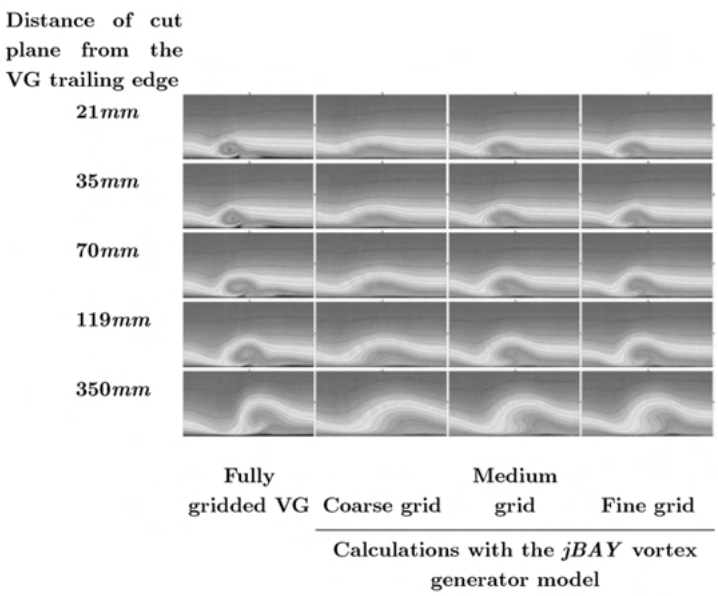

Figure 11 – jBAY VG model, three different grids in right columns, compared with gridded solution, leftmost column. From Jirasek, [6]

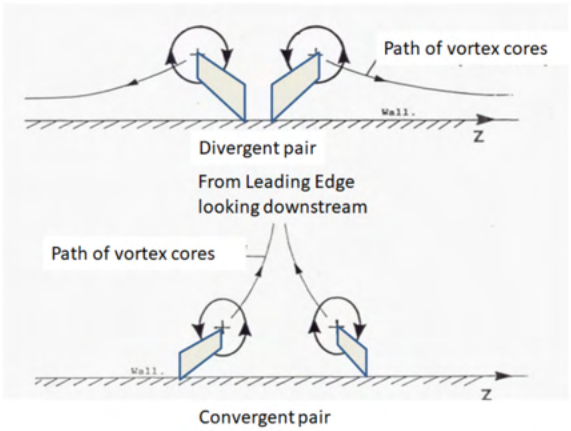

Figure 12 – Convergent and divergent VG pairs create uplift and downwash, viz., on the vortex.

4. Computed flows and conclusions

A sweep of incidence from 10 to 20 degrees at $M_\infty = 0.5$ was computed with RANS and Spalart-Allmaras turbulence model. Lift and moment curves were shown above, showing the beneficial effect. Fig. 14 investigates the flow field at α 18° by surface C_p and various vortex visualizations. Top: pressure coefficient in a $x = const$ plane. The VGs on the right wing create the pressure wiggles on the leading edge. They create a more concentrated vortex further outboard with lower surface pressure. The decrease is easily seen by counting the iso-curves.

Bottom left shows iso-surfaces of the Q_2 vorticity criterion, the threshold chosen to show the vortex onsets clearly. The label "vortex splitter" is very appropriate.

Bottom right clarifies how VGs (right wing) keep the vortex more upstream and more compact so the right wingtip has more lift.

Even the very serious study of UCAV wing shape parameters by Hövelmann [9] finds quite limited improvements for most modifications attempted. VGs were not tried in that study, and the CFD simulations reported here show that VGs can improve stall characteristics by some small amount. It is clear that an optimization of VG positions is necessary to map out how much can be achieved and what the cost in terms of drag is.

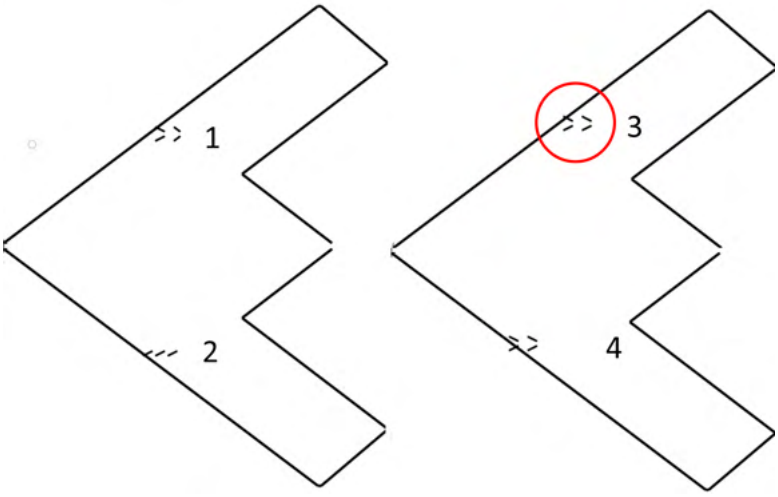

Figure 13 – Four different arrangements, top right gave best result

5. Contact Author Email Address

Mailto: peter.eliasson2@saabgroup.com

6. Copyright Statement

References

[1] Cummings, R., Schütte, A. Integrated Computational/Experimental Approach to Unmanned Combat Air Vehicle Stability and Control Estimation. *Journal of Aircraft*, Vol. 49, No. 6, November-December, pp. 1542-1557, 2012.

[2] Schütte, A., Hummel, D., Hitzel, S.: Flow Physics Analyses of a Generic Unmanned Combat Aerial Vehicle Configuration, *Journal of Aircraft*, Vol. 49, No. 6, November-December, pp. 1638-1651, 2012.

[3] Palme, H.O. (1953) Summary of Stalling Characteristics and Maximum Lift of Wings at Low Speeds, *Saab Technical Notes TN-15*, Linköping, 1953.

[4] Kuchemann, D. Types of Flow on Swept Wings, *J. Royal Aeronautical Soc*, Nov. 1953.

[5] Wendt,B.J, Greber,I., and Hingst,W.R., The Structure and Development of Streamwise Vortex Arrays Embedded in a Turbulent Boundary Layer, *NASA Technical Memorandum 105211*, September 1991

[6] Jirasek, A., Modeling Vortex Generators in a Navier-Stokes Code, *Journal of Aircraft*, Vol. 42, No. 6, November-December 2005

[7] Dudek, J.C., Modeling Vortex Generators in a Navier-Stokes Code, *AIAA JOURNAL*, Vol. 49, No. 4, April 2011

[8] Bender, E.E., Anderson, B.H., and Yagle, P. J., Vortex Generator Modeling for Navier- Stokes Codes, *Am. Soc. of Mechanical Engineers Paper FEDSM99-6929*, New York, July 1999.

[9] Hövelmann, A.N., Analysis and Control of Partly-Developed Leading-Edge Vortices *PhD Thesis*, TECHNISCHE UNIVERSITÄT MÜNCHEN, March 2016.

[10] Eliasson, P., and Weinerfelt, P.,Recent Applications of the Flow Solver Edge, *Proc. of 7:th Asian CFD Conference*, Bangalore, India, 2007.

[11] Eliasson, P., Weinerfelt, P., and Bramkamp, F., Enhancing CFD predictions for the Gripen Aircraft *International Council of the Aeronautical Sciences, ICAS*, Stockholm, 2022.

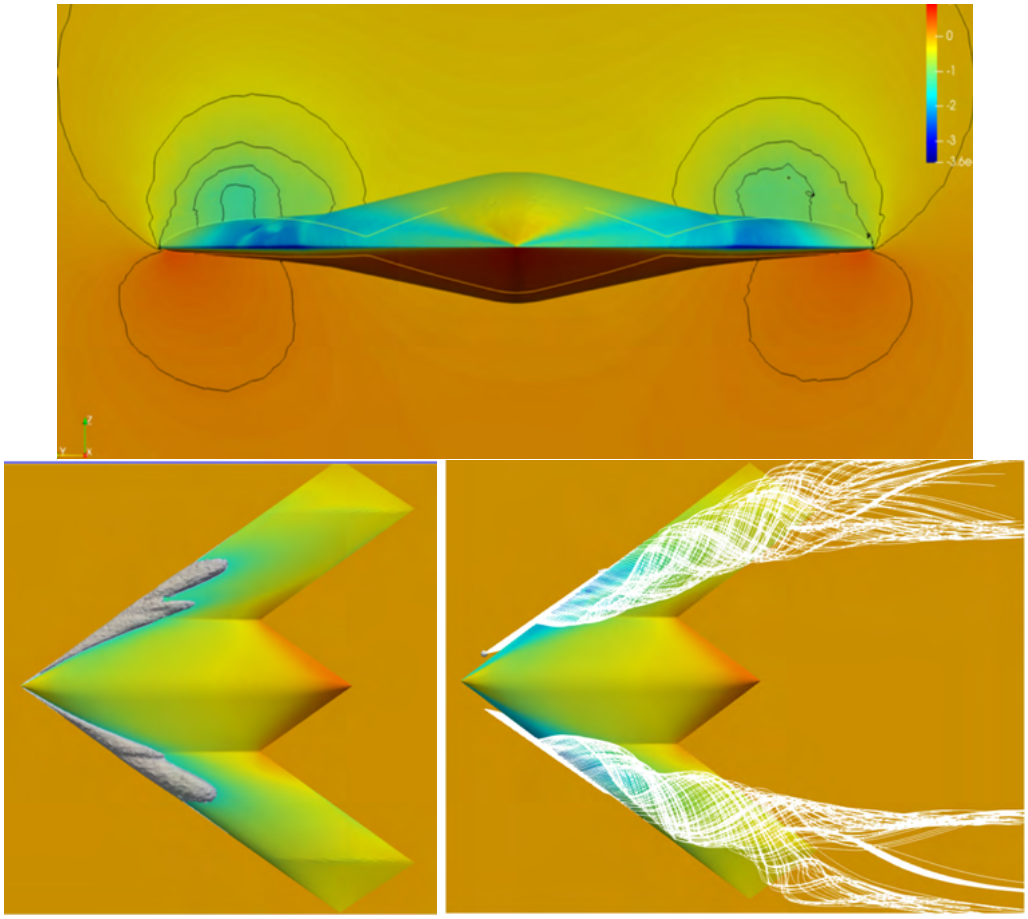

Figure 14 – Pressure coefficient on SACCON with VGs on right wing. Top, pressure in $x = const.$, Count the iso-curves! Bottom left, isosurfaces of Q_2 vorticity criterion, and bottom right, leading edge vortex streamlines. Compare patterns over left and right wing tips.